Effect to the capillary force on force measurements in submerged micromanipulations.

Mourad Nourine, Michaël Gauthier

Effect of the Capillary Force on Force Measurements in Submerged Micromanipulations

Mourad Nourine and Michael Gauthier
Laboratoire d'Automatique de Besançon: UFC, ENSMM, CNRS.
24, rue Alain Savary - 25000 Besançon - France
Tel: +33 (0) 381 402 810 - Fax: +33 (0) 381 402 809
Website: http://www.lab.cnrs.fr, E-mail: michael.gauthier@ens2m.fr

***Abstract*— The subject of this article is to analyse the impact of liquid surface tension on force measurement in submerged micromanipulations. On the one hand, at the present, mechanical characterization of biological objects in biological liquid has significant interest. On the other hand, the reduction of the surface force, and adhesion forces in a submerged medium could be a good approach to perform reliable artificial objects micromanipulations. In both cases, the micro-nano force measurement in a liquid is a great challenge. In case of a force sensor placed out of the liquid, the measurement is disturbed by the liquid surface tension. This article proposes an analysis of the disturbance of the surface tension on the force measurement. Some design rules are proposed to reduce disturbances. We shows that the major disturbances are induced by the contact angle hysteresis and a complete method is proposed to calculate these disturbances in a micromanipulation task.**

I. Introduction

Submerged micromanipulations could be divided into two types: the biological micromanipulations and the artificial submerged micromanipulations. Both micromanipulations have different constrains like biocompatibility, temperature regulation or corrosion. However this study on force measurement in liquid is general enough to be applied in both types of submerged robotic micromanipulations.

Firstly, micromanipulations of biological objects have significant interest in biotechnology. Moreover measurement of forces and mechanical properties on cell is a relevant research activity. It is indeed well established that mechanical constrains applied to cells affect their elementary biological functions [1], [2], [3]. The study of the interaction between biological properties and mechanical properties need to measure experimental microforce in the biological liquid.

Secondly, the micromanipulation and microassembly of artificial objects could be performed in liquid too: as the complexity of microsystems is always higher, new fabrication technologies of complex and/or hybrid microsystems is needed. The robotic micro-assembly is a solution to perform fabrication of new generation of microsystems [4]. An assembly task needs to be able to manipulate micro-object with a good repeatability and efficiency. The actual micromanipulation strategies are limited by the adhesion and surface effects (pull-off, van-der-Waals, electrostatic, capillary) and no reliable strategies is performed under fifty micrometers [5], [6]. To reduce this physical limit, a solution is to change the environment and to manipulate object in a liquid medium. The liquid medium (water, oil, etc.) reduces effectively significantly the adhesion and surface forces [7]. The robotic micromanipulation of artificial objects need although the measurement of the force applied on the object to preserve it [8], [9].

To summarize in cases of biomicromanipulation and submerged microassembly, microforces measurement in a liquid is at the present a critical step.

As the liquid medium could be small, it could be attractive to placed the force sensor outside of the medium (see in figure 1(a)). In that case, the force sensor measures the sum of the microforce applied by the micromanipulator on the objects (desired force) and the surface tension force applied by the liquid surface. Consequently, the measure is disturbed by the surface tension force.
In case of a submerged force sensor, the force measurement is not disturbed by the surface tension (see in figure 1(b)). Thus, the position of the force sensor (submerged or not) has an influence on the force measurement precision.
The objective of this article is to propose a general method to calculate the disturbances of the surface tension. This disturbances calculation will consist in a criteria to choose a right sensor position for a micromanipulation application (submerged or not). This article focuses neither on a specific application (biological objects, micro-assembly) nor on specific micro-object dimensions (one, ten, hundred micrometers) but proposes intentionally a general approach which can be used in large application domains. The presentation and the comparison of force measurement technologies in liquid and air medium are not in the scope of this article.

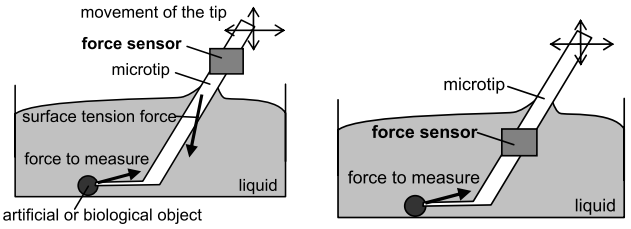

(a) Non-submerged Force Sensor (b) Submerged Force Sensor

Fig. 1. General Architecture of the Force Measurement in Submerged Micromanipulation with an External Force Sensor

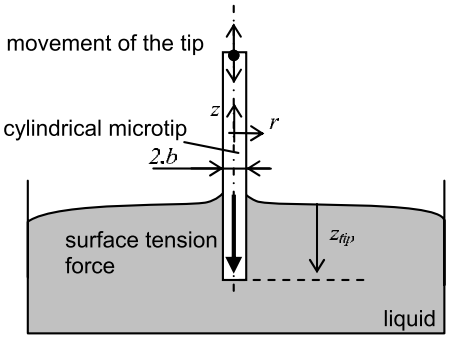

Fig. 2. Case of the Study

II. Impact of the Capillary Force

The disturbance on force measurement is not induced by the 'global' value of capillary force but especially by variations of capillary force when the micromanipulator is submerged. The 'global' value could be easily eliminated by a resetting just after the submersion. We reduce this study to a vertical cylindrical micromanipulator, and we focus on the vertical force measurement (see in figure 2).

A. Definition of the Capillary Force

The capillary force F_{cap} applied to a tip with a radius b and a perimeter $p = 2\pi b$ is:

$$F_{cap} = -p\gamma_l \cos\theta \quad (1)$$
$$\text{with} \begin{cases} \gamma_l \text{ the liquid surface tension} \\ \theta \text{ the contact angle} \end{cases}$$

The total force F applied on the tip is the sum of the weight mg, the archimede force $-F_a$, and the capillary force:

$$F = mg - p\gamma_l \cos\theta + F_a \quad (2)$$

In the microscale, volumic effect like archimede force and weight could be neglected compared to surface force like capillary force. Consequently, the equation (2) in the microscale is equivalent to:

$$F = -p\gamma_l \cos\theta \quad (3)$$

This equation shows that the force is a function of three parameters: the perimeter p of the tip near to the surface air-liquid, the surface tension of the liquid γ_l, and the angle contact θ.

The aim of this study is to analyse the influence of the variation ΔF of the force F applied to the tip on the force measurement. In the following, we study the impact of the variation of the three parameters on the force F.

The relative variation ΔF is done by:

$$\frac{\Delta F}{F} = \frac{\Delta p}{p} + \frac{\Delta \gamma_l}{\gamma_l} + \frac{\Delta \cos\theta}{\cos\theta} \quad (4)$$

We will analyse the impact of each parameter in the following sections.

B. Impact of the Perimeter

The variation of the perimeter Δp is directly function of the tip shape. To cancel this variation, the shape of the tip must be regular near to the surface air-liquid. The cancelling of this parameter gives a criteria of tip design. It is relatively easy to cancel this term. Thus the variation of the global force is done only by the variations of the surface tension and the contact angle.

C. Impact of the Surface Tension

The surface tension is a function of the liquid chemical composition and the temperature. We assume that the chemical composition of the liquid is a constant in a submerged micromanipulation. Thus the variation of the surface tension γ_l is directly a function of the liquid temperature. The surface tension typically reduces when the temperature increases. This surface tension variation is typically done by:

$$\gamma_l(T) = \gamma_l(T_0)\left[1 - \delta(T - T_0)\right] \quad (5)$$

where δ the relative thermal variation rate of the surface tension defined by:

$$\delta = -\frac{1}{\gamma_l}\frac{\partial \gamma_l}{\partial T} \quad (6)$$

Some variation rate δ are described in the table I. Values are in the order of 10^{-4} to 10^{-3}. These positive values confirm that the surface tension decreases when the temperature increases. The relative variation of the surface tension in function of the temperature is done by:

$$\frac{\Delta \gamma_l}{\gamma_l} = -\delta \Delta T \quad (7)$$

For example, in case of water, the average relative thermal variation rate δ on the range $[0; 40^oC]$ is:

$$\delta = 2.1 \times 10^{-3}\, K^{-1} \quad (8)$$

As example, a large temperature variation $\Delta T = 10^oC$ induces a relative variation of the surface tension:

$$\frac{\Delta \gamma_l}{\gamma_l} = -0.021 \quad \text{from (7)} \quad (9)$$

Consequently the variation of the temperature is able to disturb the measurement of the force applied on a tip. However, to reduce the impact of the temperature, a control of this physical parameter could be performed.

TABLE I
TYPICAL RELATIVE THERMAL VARIATION RATES OF THE SURFACE TENSION: b

liquid type	surface tension γ_l $(mN.m^{-1})$	δ (K^{-1})
water	72	$\simeq$ 0,0021
silicon oil	20	$\simeq$ 0,001
organic liquid	500	0,0001 to 0,001

D. Impact of the Surface Angle

In case of an ideal solid surface, the contact angle is a unique value [10]. Experimentally, the solid surface are heterogeneous and rough, thus the contact angle takes different values contained between an advancing angle θ_a and a receding angle θ_r. This hysteresis phenomenon has two major origins: the chemical imperfection and the roughness of the solid surface.

Some examples of contact angle hysteresis values are reported in the table II. In this table, the advancing angle and the receding angle are significantly different and shows that the advancing angle is higher than the receding angle.

TABLE II
EXAMPLES OF CONTACT ANGLE HYSTERESIS CYCLE

Liquid	Solid	θ_a / θ_r (deg)	$\frac{\Delta \cos\theta}{\cos\theta}$	
Water	Polypropylene	109 / 80	2.0	[11]
Water	Ruby	65 / 30	0.69	[12]
Water	Glass	41 / 30	0.14	[13]
nHexane	Coated-silicon	53 / 41	0.23	[14]

The uncertainties $\Delta \cos\theta / \cos\theta$ reported in the table II are very high compared to the temperature disturbances (eg. equation (9)). Consequently, the major capillary force variation is done by the hysteresis of the contact angle. Now, the measurement of the contact angle during submerged micromanipulations requires some specific vision system in a very small space. It is relatively difficult even impossible to measure in real time the variation of the contact angle in an experimental micromanipulation system.

In conclusion, in case of a force measurement in submerged micromanipulation task, the variation of the capillary force induced by contact angle hysteresis could not be neglected, and could not measured. The impact of this disturbance on the force measurement is a function of the liquid and of the micromanipulator shape and wettability.

E. Synthesis of the Variations

The variation of the capillary force in submerged micromanipulations is a sum of three elements: the variation of the micromanipulator perimeter, the variation of the liquid surface tension, the variation of the contact angle. In specific conditions, we show that the two first parameters could be neglected compared to the third element. To avoid variations of the micromanipulator perimeter, the solution is to build a micromanipulator with a regular shape. A control of the liquid temperature is able to reduce significantly the variation of the liquid surface tension. Unfortunately, the variation of the contact angle could not be neglected.

The description and model of the impact of this phenomenon on force measurement in submerged micromanipulation is described in the next section.

III. IMPACT OF THE CAPILLARY ANGLE HYSTERESIS

The impact of the capillary angle hysteresis is presented in the three following sections. First, the physical phenomenon is summarized from the literature [10-14]. Secondly, the modelling of this phenomenon based on equations presented in [10] and applied to our specific problem is proposed. Third, the impact of capillary angle hysteresis on submerged micromanipulations is discussed.

A. Presentation of the Phenomenon

To neglected the impact of its edge, we assume that the basin is large enough compared to the capillary length:

$$l_c = \sqrt{\frac{\gamma_l}{\rho_l . g}} \qquad (10)$$

with $\begin{cases} \rho_l \text{: the liquid density} \\ g \text{: the gravity} \end{cases}$

We note z_{tip} the opposite of the altitude of the micromanipulator (see in figure 2). We assume that the perimeter p of the micromanipulator is constant near to the liquid surface, and that the temperature is constant. The capillary force applied on the micromanipulator during an advancing-receding trajectory is presented in figure 3.

First the micromanipulator goes down (mark A on figure 3) and touch the liquid surface (mark B). From mark B to mark C, the micromanipulator is pushed in the liquid: the contact angle reaches the extreme value θ_a, and the capillary force stays constant. When the micromanipulator goes back, the contact angle increases gradually from θ_a to θ_r: the capillary force increases too (from mark C to mark D). From mark D to mark E, the micromanipulator carries on moving, the contact angle has reached the extreme value θ_r and the capillary force is constant. To finish, the contact between the micromanipulator and the liquid is broken (mark E) and the force is cancelled (mark F).

We note F_{ar} the difference between the advancing force F_a and the receding force F_r. We note z_{ar} the distance covered by the manipulator between the marks C and D. The modelling of this curve and the analysis of the impact of this hysteresis cycle in submerged micromanipulation is presented in the following.

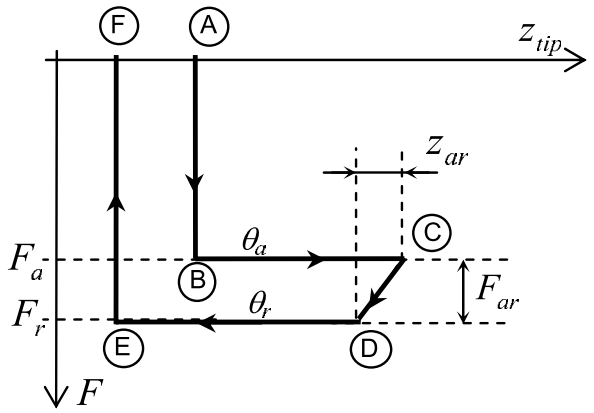

Fig. 3. Presentation of Capillary Angle Hysteresis

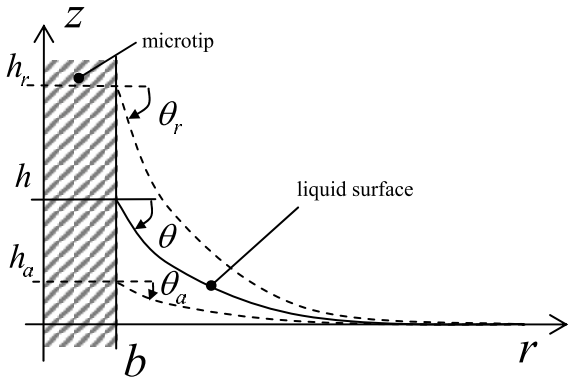

Fig. 4. Meniscus Shapes

B. Modelling

The aim of this part is to compute classical model of the capillary forces to obtain an analytic model of the parameters z_{ar} and F_{ar}.

1) Determination of F_{ar}: parameter F_{ar} is obtain thanks to the definition of the capillary force described in equation (1):

$$F_{ar} = F_a - F_r = -p\gamma_l(\cos\theta_a - \cos\theta_r) \tag{11}$$

This parameter could be calculated in function of the geometry of the tip, the surface tension, and the surface angles.

2) Determination of z_{ar}: on the arc 'CD' on the figure 3, the contact line between the liquid surface and the tip is fixed. The contact angle varied from the value θ_a to θ_r. The distance z_{ar} represents the displacement of the tip to increase θ from θ_a to θ_r. We note h_a and h_r the height of the liquid meniscus respectively in case of θ_a and θ_r. Consequently:

$$z_{ar} = h_r - h_a \tag{12}$$

To determine the value of z_{ar}, the value of the height h of the meniscus has to be expressed in function of the contact angle θ.

The meniscus shape is described in figure 4. Classical capillary studies are able to prove that the meniscus shape is defined by [10]:

$$r = b'.\cosh\left(\frac{h'-z}{b'}\right) \tag{13}$$

Now, in our case:

$$r = b \Rightarrow \begin{cases} z = h \\ \frac{dr}{dz} = -tan(\theta) \end{cases} \tag{14}$$

So:

$$r = b.\cos\theta.\cosh\left(\frac{-z + h + b.\text{acosh}\left(\frac{1}{\cos\theta}\right).\cos\theta}{b.\cos\theta}\right) \tag{15}$$

The length of the meniscus is currently defined by the capillary length l_c (10) so:

$$r = l_c \Rightarrow z = 0 \tag{16}$$

consequently:

$$h = b\cos\theta\left[\text{acosh}\left(\frac{l_c}{b.\cos\theta}\right) - \text{acosh}\left(\frac{1}{\cos\theta}\right)\right] \tag{17}$$

From (12) and (17), the parameter z_{ar} is so defined by:

$$\begin{aligned} z_{ar} = {} & b\cos\theta_r\left[\text{acosh}\left(\frac{l_c}{b.\cos\theta_r}\right) - \text{acosh}\left(\frac{1}{\cos\theta_r}\right)\right] \\ & - b\cos\theta_a\left[\text{acosh}\left(\frac{l_c}{b.\cos\theta_a}\right) - \text{acosh}\left(\frac{1}{\cos\theta_a}\right)\right] \end{aligned} \tag{18}$$

Characteristic parameters F_{ar} and z_{ar} of the hysteresis cycle (figure 3) are defined by the equations (11) and (18).

C. Impact on a Micromanipulation Task

The aim of this part is to present the variation of the capillary force ΔF induced by the capillary angle hysteresis. We differentiate two cases in function of the vertical movement Δz required by the tip:

- case of large vertical movement: $\Delta z \geq z_{ar}$
- case of small vertical movement: $\Delta z < z_{ar}$

In case of large vertical movement, the capillary force F varies from F_a to F_r and the variation of the capillary force is then:

$$\Delta z \geq z_{ar} \Rightarrow \Delta F = F_{ar} = 2\pi b\gamma_l(\cos\theta_a - \cos\theta_r) \tag{19}$$

In case of small vertical movement, the capillary force F does not vary on the complete interval $[F_a, F_r]$. Consequently the variation of F is smaller than F_{ar} and is a function of the vertical movement Δz. The force F described the arc 'CD' during the vertical tip movement. The arc 'CD' is defined by the equation:

$$\begin{aligned} z_{tip} &= -(h - h_a) + z_a \quad \text{with: } z_a = \text{constant} \\ &= \frac{F}{2\pi\gamma_l}\left[\text{acosh}\left(\frac{2\pi l_c\gamma_l}{-F}\right) - \text{acosh}\left(\frac{p\gamma_l}{-F}\right)\right] + h_a + z_a \end{aligned} \tag{20}$$

In case of water, the simulated arc 'CD' described by (20) is presented in the figure 5. The arc 'CD' presented in figure 5 is relatively comparable to an affine function. Consequently the derivative $\frac{dF}{dz}(CD)$ on the arc 'CD' could be approximated by a constant value:

$$\frac{dF}{dz}(CD) \simeq \frac{F_a - F_r}{-(h_a - h_r)} \tag{21}$$

$$\simeq 2\pi b\gamma_l \frac{\cos\theta_a - \cos\theta_r}{z_{ar}} \tag{22}$$

Consequently the variation ΔF is approximated by:

$$\Delta F = \frac{dF}{dz}(CD)\Delta z \tag{23}$$

So from equation (22):

$$\Delta z < z_{ar} \Rightarrow \Delta F = 2\pi b\gamma_l(\cos\theta_a - \cos\theta_r)\frac{\Delta z}{z_{ar}} \tag{24}$$

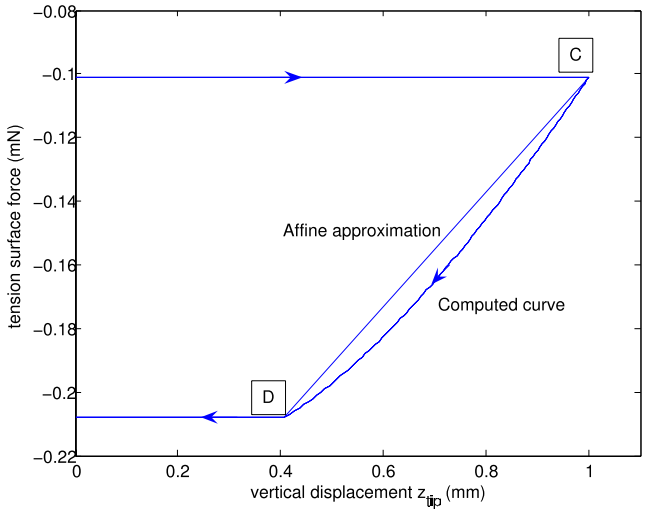

Fig. 5. Simulated Arc 'CD' and Affine Approximation

The equations (19) and (24) give a model of the disturbance ΔF on force measurement in function of the vertical range of the tip displacement Δz, the radius b of the tip, the surface tension γ_l, and the contact angles θ_a, θ_r.

IV. Experimentations

To validate experimentally the force disturbance model, some experimentations were done.

A. Measurement Device

The experimental force measurement device is described in the figure 6. The measurement of the force is performed by a precision balance which is able to measure surface tension forces (around hundreds micro Newtons). Water is in a standard petri box whose diameter (3 in.) is larger that the capillary length l_c. The petri box is placed on a motorize micropositionning stage (Physik Instrument, PI-M-112.1-DG). The glass microtip is fixed to the microbalance to measure surface force. The relative position between surface water and the tip is controlled by the micropositionning system.

Relative displacements, and measured forces are recorded by a computer.

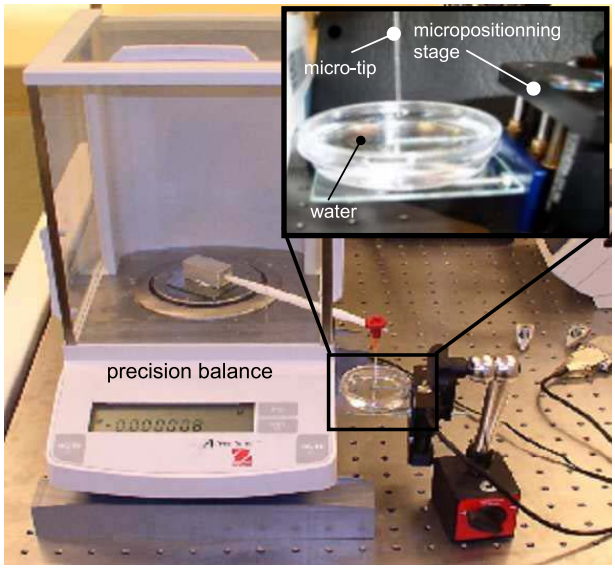

Fig. 6. Experimental Measurement Device of Capillary Force

B. Experimental Force Measurement

The radius of the glass tip is $b = 475\,\mu m$. The experimental temperature is $T = 20^oC$, consequently $\gamma_l = 72.8\,mNm^{-1}$.

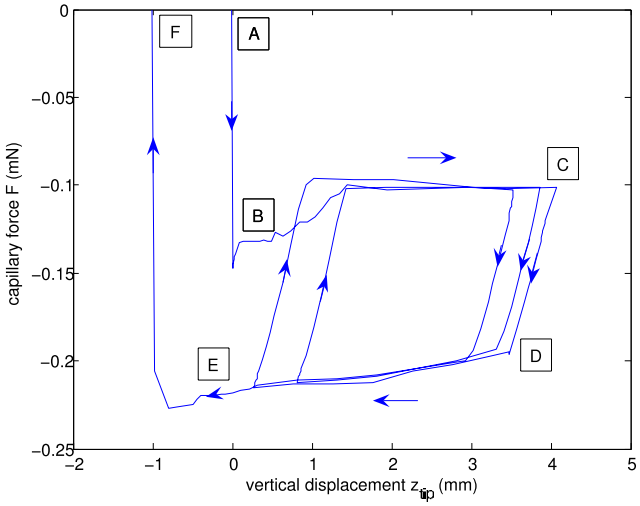

Fig. 7. Experimental Measurement of a Capillary Hysteresis Cycle

The experimental capillary hysteresis cycle presented in figure 7 is near to the theoretical curve (see in figure 3). The penetration of the liquid takes place in mark A. The major differences between experimental measurement and theory appear just after the contact (mark B). These differences are induced by the shape of the bottom of

the glass tip. Effectively, at the bottom, the glass tip has no constant radius b. This effect was not taken into account in the theory. Some advancing-receding cycles (marks B-C-D-E) were made at different altitude z and show a relatively good repeatability. The affine function seems to be a good approximation of the arc 'CD'. This hypothesis is validated by the experiments. Finally, some force increasing is observed just before the exit of the liquid (mark E). This phenomenon is explained by the bottom shape of the tip (like mark B).

The experimental values measured on the figure 7 are:

$$\begin{cases} z_{ar} & = 575 \pm 180\,\mu m \\ F_a & = 101 \pm 5\,\mu N \\ F_r & = 208 \pm 10\,\mu N \end{cases} \tag{25}$$

From (3), we determine θ_a, and θ_r:

$$\theta_a = 62.3 \pm 1.5\,\text{deg} \tag{26}$$

$$\theta_r = 17.3 \pm 9\,\text{deg} \tag{27}$$

These angle values obtained from the force measurement is in the same order of values as angle hysteresis described in table I. The value of the measured force is then validated.

By using these experimental values of contact angles in (18) we obtain:

$$z_{ar} = 582 \pm 120\,\mu m \tag{28}$$

The measured z_{ar} (25) and the recalculated z_{ar} (28) are relatively near.

Experiments show a good relevance of force disturbance measurement and theoretical study. Consequently the force disturbance model (19), (24) is validated.

Consequently, in case of the design of a micromanipulation station for a specific application, this general method is able to produce design criteria choosing the position of the force sensor (submerged or not).

V. Conclusion

As the micromanipulation in liquid has interest in biological application and in mechatronics application, micro-nanoforces measurements in submerged micromanipulations have significant interest. We propose some design rule (tip regular shape, temperature regulation) to reduce the impact of the capillary. We show that the force measurement in submerged medium could be highly disturbed by the contact angle hysteresis. A complete model of the capillary disturbances on force measurement was presented. A method was proposed to calculate the disturbance on the force measurement in function of the vertical displacement of the tip, the radius of the tip, the surface tension of the liquid, the contact angles. The determination of this disturbance could determine the position (submerged or not) of a force sensor for specific micromanipulation applications. Further works will focus on the expression on this disturbance in a more complex and realistic architecture.

References

[1] Z. Yihua, W. Berns, S. Usaml, R. Tslen, W. Yingxiao, E. Botvinick, and C. Shu., "Visualizing the mechanical activation of src," *Nature*, vol. 434, pp. 1040–1045, 2005.

[2] K. Podyma-Inoue, M. Yanagishita, S. Ozaki, S. Kaneko, and K. Soma., "Modulation of extracellular matrix synthesis and alkaline phosphatase activity of periodontal ligament cells by mechanical stress." *Journal of periodontal research*, vol. 40, no. 2, pp. 110–117, 2005.

[3] J. Park, S.-H. Jung, Y.-H. Kim, B. Kim, S.-K. Lee, B. Ju, and K.-I. Lee, "An integrated bio cell processor for single embryo cell manipulation," in *Proceedings of 2004 IEEE/RSJ International Conference on Intelligent Robots and Systems*, Sendai, Japan, Oct. 2004, pp. 242–45.

[4] H. V. Brussel, J. Peirs, D. Reynaerts, A. Delchambre, G. Reinhart, N. Roth, M. Weck, and E. Zussman, "Assembly of microsystems," *Annals of the CIRP*, vol. 49, no. 2, pp. 451–472, 2000.

[5] T. Udeshi and K. Tsui, "Assembly sequence planning for automated micro assembly," in *International Symposium on Assembly and Task Planning*, 2005.

[6] N. Dechev, W. L. Cleghorn, and J. K. Mills, "Microassembly of 3d microstructures using a compliant, passive microgripper," *Journal of Microelectromechanical Systems*, vol. 13, no. 2, April 2004.

[7] J. Israelachvili, *Intermolecular and Surface Forces*. Academic Press, 1991.

[8] M. Gauthier, B. Lopez-Walle, and C. Clévy, "Comparison between micro-objects manipulations in dry and liquid mediums," in *proc. of CIRA'05*, June 2005.

[9] M. Gauthier, S. Régnier, P. Rougeot, and N. Chaillet, "Forces analysis for micromanipulations in dry and liquid media," *Journal of Micromechatronics*, accepted nov. 05 2006.

[10] P.-J. D. Gennes, F. Brochard-Wyart, and D. Quéré, *Gouttes, bulles, perles et ondes*. Edition Belin, 2002.

[11] C. D. Volpe, D. Maniglio, S. Siboni, and M. Morra, "An experimental procedure to obtain the equilibrium contact angle from wilhelmy method," *Oil and Gas Science and technlogy*, vol. 56, pp. 9–22, 2001.

[12] O. Pitois and X. Chateau, "Small particle at a fluid interface: effect of contact angle hysteresis on force and work detachment," *Langmuir*, vol. 18, pp. 9751–56, 2002.

[13] R. H. Dettre and R. E. Johnson, "Contact angle hysteresis iv contact angle measurements on heteorogenous surfaces," *The journal of physical chemistry*, vol. 69, no. 5, 1965.

[14] C. Lam, N. Kim, D. Hui, D. Kwok, M. Hair, and A. Neumann, "The effect of liquid properties to contact angle hysteresis," *Colloids and Surfaces A: Physicochemical and Engineering Aspects*, vol. 189, pp. 265–278, 2001.